Discovery of Native Metal Ion Sites Located on the Ferredoxin Docking Side of Photosystem I[†]

Lisa M. Utschig,* Lin X. Chen, and Oleg G. Poluektov

Chemical Sciences and Engineering Division, Argonne National Laboratory, Argonne, Illinois 60439

Received January 8, 2008

ABSTRACT: Photosystem I (PSI) is a large membrane protein that catalyzes light-driven electron transfer across the thylakoid membrane from plastocyanin located in the lumen to ferredoxin in the stroma. Metal analysis reveals that PSI isolated from the cyanobacterial membranes of *Synechococcus leopoliensis*has a near-stoichiometric 1 molar equiv of Zn^{2+} per PSI monomer and two additional surface metal ion sites that favor Cu^{2+} binding. Two-dimensional hyperfine sublevel correlation (HYSCORE) spectroscopy reveals coupling to the so-called remote nitrogen of a single histidine coordinated to one of the Cu^{2+} centers. EPR and X-ray absorption fine structure (XAFS) studies of 2Cu−PSI complexes reveal the direct interaction of ferredoxin with the Cu^{2+} centers on PSI, establishing the location of native metal sites on the ferredoxin docking side of PSI. On the basis of these spectroscopic results and previously reported site-directed mutagenesis studies, inspection of the PSI crystal structure reveals a cluster of three highly conserved residues, His(D95), Glu(D103), and Asp(C23), as a likely Cu^{2+} binding site. The discovery of surface metal sites on the acceptor side of PSI provides a unique opportunity to probe the stromal region of PSI and the interactions of PSI with its reaction partner, the soluble electron carrier protein ferredoxin.

Photosynthetic reaction center proteins (RCs)[1] are finely tuned molecular systems optimized for solar energy conversion. In RCs, photoinduced rapid, sequential electron transfer reactions result in the formation of a charge-separated state that is linked to important secondary reaction sequences, such as proton transfer or electron transfer with mobile charge carriers. Previously, we discovered a surface metal ion site on the purple photosynthetic bacterial RC (bRC) that modulates proton-coupled electron transfer (*1, 2*). In bRCs, light-induced electron transfer terminates in the electron transfer between two quinone molecules, Q_A and Q_B, and this electron transfer reaction is coupled to proton uptake. Zn^{2+} binds near the protein surface to a site located ∼18 Å below the Q_B binding pocket (*3*) and slows interquinone electron transfer (*1*) and proton uptake by Q_B (*4*). Subsequently, proton gateways in the bRC (*5*) and other proteins have been identified via surface Zn^{2+} sites (*6*). The importance of surface Zn^{2+} protein sites has led us to examine the possibility that such metal ion sites exist in the photosystem I (PSI) RC.

In oxygenic photosynthesis of higher plants, cyanobacteria, and algae, PSI catalyzes light-driven electron transfer across the thylakoid membrane from plastocyanin located in the lumen to ferredoxin in the stroma (*7, 8*). PSI is a large, membrane protein complex composed of 12 protein subunits and 127 cofactors. In PSI, photoexcitation of the primary electron donor, P700 (a dimer of cholorophyll molecules), initiates electron transfer to two spectroscopically identified electron acceptors, A_0, a chlorophyll molecule, and A_1, a phylloquinone. From A_1^-, the electron is transferred to the [4Fe-4S] cluster F_X, and further to F_A and F_B, two [4Fe-4S] clusters held within the extrinsic protein subunit PsaC. The electron is then transferred to ferredoxin, a small [2Fe-2S] protein that shuttles the reducing equivalents from PSI to several metabolic pathways. Three protein subunits, PsaC, PsaD, and PsaE, form the stromal hump of PSI and are involved in the docking of ferredoxin (*7–9*). To date, the only reported transition metal ion in PSI is the Fe found in the clusters. Herein, we report the discovery of native surface metal ion sites on the acceptor side of the PSI RC and provide spectroscopic evidence of the interaction of these sites with the soluble electron carrier protein ferredoxin.

EXPERIMENTAL PROCEDURES

Purification of Photosystem I. Cells of *Synechococcus leopoliensis* (UTEX625) were grown in Ac medium (*10*) at ∼40 °C. Thylakoid membranes and PSI complexes were prepared according to the procedures of Rögner et al. (*11*). PSI was purified through the sucrose gradient step; additional chromatography steps that might strip native bound metal ions from PSI were eliminated. The lower dark green band from the sucrose gradient was dialyzed overnight into 20 mM Hepes (pH 7.9), 25 mM $MgSO_4$, and 0.03% β-DM (*n*-dodecyl β-D-maltopyranoside, Anatrace) and concentrated with Centriprep-50 (Amicon) devices. PSI purified with Tris/

[†] This work was supported by the U.S. Department of Energy, Office of Basic Energy Sciences, Division of Chemical Sciences, Geosciences, and Biosciences, under Contract DE-AC02–06CH11357. Use of the Advanced Photon Source was supported by the U.S. Department of Energy, Office of Science, Office of Basic Energy Sciences, under Contract DE-AC02-06CH11357.

* To whom correspondence should be addressed. Phone: (630) 252-3544. Fax: (630) 252-9289. E-mail: utschig@anl.gov.

[1] Abbreviations: RC, reaction center; bRC, bacterial reaction center; PSI, photosystem I; HYSCORE, two-dimensional hyperfine sublevel correlation; EPR, electron paramagnetic resonance; XAFS, X-ray absorption fine structure; cw, continuous wave; ESE, electron spin–echo.

10.1021/bi800038d CCC: $40.75
Published on Web 02/23/2008

Triton-based sucrose preparations (*12*) contained ~0.3 Zn ion per PSI. Chlorophyll was assessed in 100% methanol by measuring the optical density at 664 nm (*13*). P700 was assessed by chemical difference spectroscopy (*14*). Purified PSI was analyzed for Zn, Cu, Mg, and Fe content as detailed below.

Binding of Cu^{2+} to PSI. The amount of native Cu present in isolated PSI was very dependent on the buffers used in the purification, with ratios ranging from 0.1 to 0.9 molar equiv of Cu per PSI monomer. Stoichiometric Cu binding can be obtained by incubating purified PSI with several equivalents of $CuSO_4$, followed by gel filtration chromatography to remove unbound metal ion (*15, 16*). Consistent Cu binding was achieved using Hepes buffer, a "Good's" buffer that has a low metal binding constant. Typically, ~6 μM PSI in 20 mM Hepes (pH 7.9), 25 mM $MgSO_4$, and 0.03% β-DM was incubated at ice temperature with 6–10 molar equiv of $CuSO_4$ (final concentration of Cu^{2+} of ~40 μM, from an 80 mM stock) for 3 h. The free Cu^{2+} was separated from bound metal ion by gel filtration chromatography through a Sephadex G-25 (Pharmacia) column equilibrated with the same buffer. Bound Cu^{2+} can be removed from PSI by overnight dialysis against 50 mM Tris-Cl (pH 8.0), 200 mM NaCl, 1 mM EDTA, and 0.03% β-DM, with several buffer changes. Native Zn^{2+} that copurifies with PSI (see below) can be removed by the same method. Centriprep-50 devices were used to concentrate Cu^{2+}−PSI samples for EPR and XAFS experiments.

Size exclusion preparation yields average Cu/PSI ratios of 2.1 ± 0.2, with 0.1 being the standard deviation due to variations between sample preparations. The cw EPR spectrum obtained for eight samples with two Cu ions per PSI, each prepared from a different purification of PSI, are essentially identical. In addition to the two Cu^{2+} ions, four of these samples analyzed by EPR had one Zn^{2+} bound to PSI (as purified); four samples had <0.3 Zn^{2+} bound. The consistency of the Cu/PSI ratios and the EPR spectra observed substantiates that Cu^{2+} binding to PSI is not adventitious when prepared under the experimental conditions detailed. Careful control of several factors, including the ionic strength and competitor ions in the buffer, equivalents of added metal ion, incubation time, and separation techniques, is necessary to eliminate adventitious binding. Future experiments aimed at correlating metal site occupancy with function will require carefully prepared stoichiometric Zn−PSI or Cu−PSI complexes and not simply PSI in buffers containing a large excess of metal ion.

Metal Analysis. Inductively coupled plasma-atomic emission spectroscopy (ICP-AES) on a Thermo Jarell Ash Atomscan Advantage spectrometer was used to determine metal content (Cu, Zn, Fe, and Mg). The ICP-AES instrument is equipped with an axial plasma configuration. The analytical standard deviation for these measurements was ~0.01. Each sample was measured for Fe content. Thus, a ratio of 12 Fe atoms per PSI proved to be self-consistent with the P700 determination for PSI concentration. Measurement of Mg content concurred with the Chl concentrations determined in methanol.

Ferredoxin Preparations. Lyophilized spinach ferredoxin (Sigma) was resuspended in 20 mM Hepes (pH 7.9), 25 mM $MgSO_4$, and 0.03% β-DM. The ferredoxin had been lyophilized in Trizma buffer, and therefore, it was essential to remove as much Trizma as possible because it can form coordination complexes with divalent metal ions. The ferredoxin was repeatedly diluted and then concentrated with microcon-3 devices to wash away the Trizma buffer. The ferredoxin concentration was determined by measuring the absorption at 423 nm (molar absorption coefficient of 9600 L mol^{-1} cm^{-1}) (*17*). Typically, 7–10 molar equiv of ferredoxin (from a 5–8 mM stock) was added to PSI and the mixture incubated on ice overnight.

EPR Measurements. X-Band (9.5 GHz) EPR measurements were carried out with a Bruker Elexsys E580 spectrometer (Bruker Biospin Corp.). For continuous wave measurements, a standard rectangular cavity was employed, and for pulsed measurements, a Bruker MD4 dielectric cavity was used. ESE-detected EPR spectra were recorded as the intensity of two pulsed ESE as a function of the magnetic field strength. The temperature was controlled by an Oxford cryostat and temperature controller. The hyperfine sublevel correlation (HYSCORE) spectra were recorded at 4.5 K. HYSCORE experiments were performed using the pulse sequence $\pi/2$–τ–$\pi/2$–t_1–π–t_2–$\pi/2$–τ–echo, with a $\pi/2$ pulse length of 16 ns and a 32 ns π pulse. Time intervals t_1 and t_2 were varied with steps of 68 ns; 128 points were collected in each dimension. A four-step phase cycle was used to eliminate unwanted echoes.

Preparation of Samples for XAFS Experiments. PSI purified with *n*-dodecyl β-D-maltopyranoside/sucrose gradient-based prep (*11*) containing one Zn per PSI was incubated with 10 equiv of $CuSO_4$ followed by size exclusion chromatography and concentrated as detailed above, to a final concentration of ~250 μM. The final metal-to-protein ratio was 2.5 Cu/0.6 Zn/12 Fe/PSI. The Cu^{2+} EPR spectrum observed for this sample was typical of spectra obtained with previous 2 Cu/PSI samples. This sample was split into two aliquots. To one aliquot, "2Cu-PSI" sample, was added glycerol, and XAFS was obtained. To the second aliquot was added ferredoxin to a final concentration of 1.5 mM. The sample was incubated overnight, followed by the addition of glycerol. This is the "2Cu-PSI-ferredoxin" sample. The third sample, "Cu/ferredoxin", was a solution containing 500 μM $CuSO_4$ and 1.5 mM ferredoxin.

XAFS Measurements. Copper K-edge X-ray absorption near edge structure (XANES) and X-ray absorption fine structure (XAFS) spectra were collected at beamline 12BM at the Advanced Photon Source of Argonne National Laboratory in a manner similar to our previous experiments (*18*). Si(111) double crystals were used in the monochromator. A Pt-coated mirror was used to focus the beam and to remove higher harmonic X-ray photons. The beam size at the sample was approximately 0.4 mm (v) × 1 mm (h). A feedback system was used to control the monochromator crystal angle and was set to 70% detuning. A 13-element germanium solid state detector (Canberra) was used to collect iron X-ray fluorescence signals. A manganese filter was placed in front of the detector for attenuation of elastic scatterings, which increased the signal ratio between the fluorescence and the elastic scattering of the sample from <1/100 to ~1/1. The outputs from the amplifiers of the detector were connected to an array of single-channel analyzers (SCA) with upper and lower thresholds set to allow only $K_{\alpha 1}$ and $K_{\alpha 2}$ fluorescence signals to be further processed. An ion chamber was placed before the sample for the incident

X-ray flux reference signal I_0, and the second and the third ion chambers were placed after the sample. A copper foil inserted between the second and third ion chambers was used for energy calibration. The output signals from the SCAs were connected to a scalar array which interfaced with a computer hosting a data acquisition program (G. Jennings, Argonne National Laboratory). Samples were placed in a disk-shaped aluminum holder with Mylar windows. The holder was attached to a close-cycle cryogenic system (Janis). The sample measurements were carried out at 15 K in dark. Data analysis was carried out using WinXAS (T. Ressler) with FeFF8.0 (University of Washington, Seattle, WA) for generating model structures and fitting (data not shown).

RESULTS

Our metal analysis of PSI isolated from cyanobacterial membranes of *S. leopoliensis* reveals that PSI has a near-stoichiometric 1 molar equiv of Zn^{2+} per PSI monomer. No Zn^{2+} was added during the purification protocol. Cells were grown with typical medium conditions, and extensive chromatography steps were eliminated from the purification procedure so that native bound metal ion would not be stripped from PSI. Ten different PSI *n*-dodecyl β-D-maltopyranoside/MES sucrose gradient preparations (*11*) were analyzed, resulting in an average ratio of 1.3 ± 0.3 Zn ions per PSI, with 0.3 being the standard deviation due to variations between sample preparations.

We initiated Cu^{2+} binding studies of PSI to spectroscopically interrogate the metal site. Cu^{2+} ion ($3d^9$, $S = {}^1/_2$) is a useful spin probe of protein metal sites, whereas Zn^{2+} is diamagnetic and cannot be detected by EPR spectroscopy. To our surprise, Cu^{2+} does not readily replace the native Zn^{2+} that copurifies with PSI but instead binds to two additional sites on PSI. Stoichiometric Cu binding (Cu to RC mole ratio of 2) can be obtained by incubating purified PSI with several equivalents of $CuSO_4$ followed by gel filtration chromatography to remove unbound metal ions (*15, 16*). Although Cu^{2+} does not readily replace the native bound Zn^{2+} ion, partial replacement can occur. Thus, in addition to the Zn^{2+} site, there are two other metal ion sites that favor Cu^{2+} binding. PSI has at least three transition metal ion sites: one favorable to Zn binding and two favorable to Cu binding. Zn^{2+} and Cu^{2+} can be removed from PSI by the addition of metal ion competitors, suggesting that the sites are surface accessible, similar to the Zn^{2+} site in bRCs that influences the terminal interquinone proton-coupled electron transfer steps (*1*).

Our initial efforts have focused on investigating the location and potential function of the paramagnetic Cu^{2+} sites in PSI. Cu^{2+} bound to PSI exhibits an axially symmetric electron paramagnetic resonance (EPR) spectrum with the following values: $g_{||} = 2.24$, $A_{||} = 175$ G, and $g_{\perp} = 2.05$ (consistent with tetragonal symmetry for the coordinated ligands) (*19*). The spectrum is typical of type 2 or "normal" copper EPR signals, having *g* and *A* values characteristic of most cupric complexes (*20*). The two Cu^{2+} centers cannot be distinguished from each other in the EPR spectrum. Most likely, the Cu^{2+} signals overlap and are not resolved, although it is possible that one Cu is either Cu^{+}, and thus diamagnetic, or a Cu^{2+} center located close to an Fe−S cluster which would significantly broaden the EPR signal. The observed

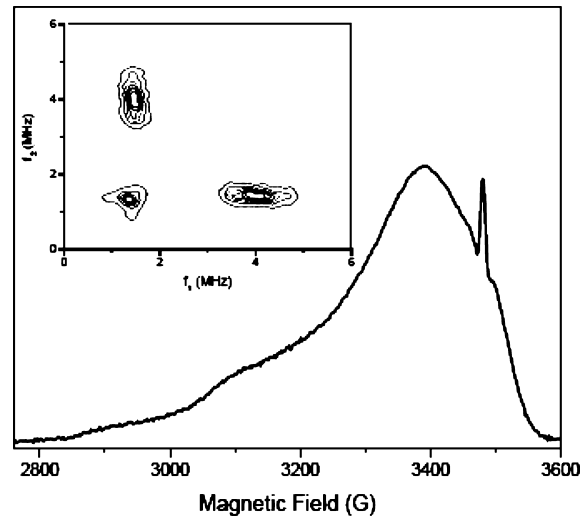

FIGURE 1: Field-swept ESE spectrum of 2Cu-PSI. The inset shows the HYSCORE spectrum of Cu^{2+} centers in PSI indicating histidine−Cu coordination. The sample contained ~40 μM PSI with a metal/protein ratio of 2.0 Cu/0.2 Zn/12 Fe/PSI. Cu-PSI was prepared by size exclusion chromatography following incubation with $CuSO_4$, as described in Experimental Procedures. The sample was dark adapted 30 min prior to being frozen in liquid N_2.

EPR spectrum is identical for 2 molar equiv of Cu^{2+} bound to PSI (2Cu-PSI) with or without Zn^{2+} bound in the native Zn^{2+} site. The Cu^{2+} EPR signal is unchanged after low-temperature illumination. Thus, the Cu^{2+} does not magnetically interact with the light-induced radical species $P^+F_A^-$ or $P^+F_B^-$ (*21*) and is not reduced to Cu^{+} following illumination. After addition of spinach ferredoxin to 2Cu-PSI, the cw EPR spectrum is broadened and the spectral parameters change ($g_{||} = 2.30$, and $A_{||} = 140$ G). These X-band EPR spectral results suggest that ferredoxin is binding at or near at least one of the Cu^{2+} centers on PSI.

Pulsed EPR spectroscopy provides the first direct structural information about the ligands in the Cu^{2+} sites of PSI. HYSCORE spectroscopy was used to measure the hyperfine and electric quadrupole interactions of weakly coupled ^{14}N nuclei (*22, 23*). The ^{14}N HYSCORE spectrum reveals coupling to the so-called remote nitrogen of a single histidine coordinated to one of the Cu^{2+} centers (Figure 1) (*15, 24*). Examination of the crystal structure of PSI (*7*) shows three histidine residues, D95, E63, and C2, on the stromal subunits. His-C2 could be a ligand; however, this histidine would not be observed spectroscopically due to significant broadening of the EPR spectrum from dipole–dipole/exchange interactions with the nearby Fe−S cluster F_A. Mutation of the highly conserved His(D95) and nearby Glu(D103) has been shown to influence ferredoxin binding (*25, 26*). Examination of the crystal structure shows that these two residues, His(D95) and Glu(D103), along with a nearby Asp(C23) residue are in the proximity of each other. Histidines, glutamates, and aspartates are common metal-binding ligands, and thus, we propose that these three highly conserved residues comprise one of the Cu^{2+} binding sites on PSI (Figure 2).

To examine in detail the influence of ferredoxin binding on the local coordination environments of Cu^{2+} sites in PSI, we have conducted Cu K-edge XAFS studies of PSI at beamline 12BM (Advanced Photon Source, Argonne National Laboratory). XAFS is a sensitive local structural probe of metal atom coordination spheres (*27*) and hence provides

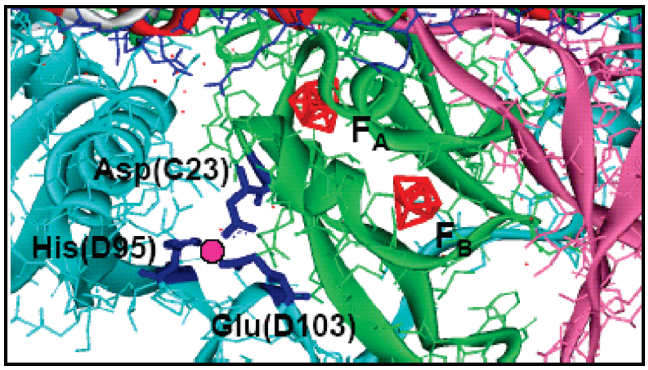

FIGURE 2: Proposed Cu^{2+} site in PSI (Protein Data Bank entry 1JB0). Enlargement of the stromal subunits PsaC (green), PsaD (cyan), and PsaE (magenta) showing the proposed Cu binding site ligands (dark blue) His(D95), Asp(C23), and Glu(D103) in PSI. A putative Cu atom is illustrated (magenta sphere).

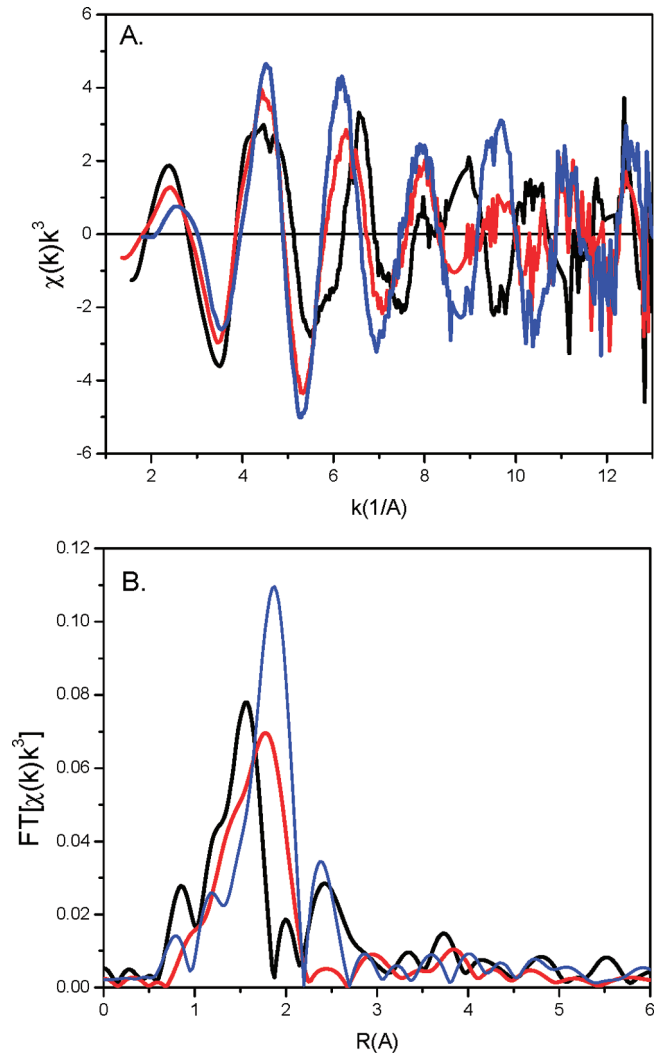

FIGURE 3: Cu K-edge (A) XAFS spectra and (B) Fourier-transformed XAFS spectra of 2Cu-PSI (black), the 2Cu-PSI−ferredoxin complex (red), and Cu/ferredoxin (blue) (without phase correction). The 2Cu-PSI and 2Cu-PSI−ferredoxin samples contained ~250 μM PSI with a final metal/protein ratio of 2.5 Cu/0.6 Zn/12 Fe/PSI. The 2Cu-PSI−ferredoxin sample contained 1.5 mM ferredoxin in addition to 2Cu-PSI. The Cu/ferredoxin sample was a solution containing 500 μM $CuSO_4$ and 1.5 mM ferredoxin.

a means of looking directly for ferredoxin-induced conformational changes in the Cu centers. Striking differences in the coordination and geometry around the Cu sites in PSI have been observed in the Cu K-edge XAFS spectra of 2Cu-PSI in the presence and absence of ferredoxin (Figure 3). Most notable is the change in the second nearest coordination shell, which is pronounced in 2Cu-PSI and Cu/ferredoxin (no PSI) but missing in the 2Cu-PSI−ferredoxin complex. This considerable spectral change is consistent with a more disordered coordination and possible loss of histidine ligation in the latter (*18*). Control experiments show that PSI retains 2 molar equiv of Cu per PSI after ferredoxin binding and exposure to X-rays. Unlike EPR, with the XAFS experiment both Cu centers will be observed in PSI, regardless of oxidation state or proximity to Fe−S centers. Thus, the XAFS results suggest that both Cu^{2+} sites are affected by ferredoxin binding. Although detailed structural parameter analysis is curtailed by the complexity associated with XAFS analysis of multiple Cu sites, the significant differences in the XAFS spectra of Cu sites in these three complexes strongly suggest that both ferredoxin and PSI contribute protein ligands to the two Cu sites in the 2Cu-PSI−ferredoxin complex. Ferredoxin has several potential metal-binding ligands, including one His, one non-Fe coordinating Cys, and a combined total of 20 Asp and Glu residues (*28*).

DISCUSSION

EPR and XAFS results establish that native Cu^{2+} sites are located on the ferredoxin docking side of PSI. Why would nature incorporate metal sites at this location? Clearly, metal ions are not required for PSI−ferredoxin docking or interprotein electron transfer (*29, 30*); however, metal ions could enhance or inhibit these processes. Thus, although the roles are not immediately obvious, the discovery of these sites provides the opportunity to capitalize on spectroscopic properties of metal ions and probe the stromal region of PSI, PSI−ferredoxin docking mechanisms, and interprotein electron transfer reactions.

Ten years after its discovery (*2*), an in vivo functional role for the bRC Zn^{2+} site remains elusive, yet this site has proven to be significant. In vitro metal binding studies of the bRC have proven to be important for elucidating the proton entry point in the bRC, the proton pathway through the bRC, and revealed a general role for surface histidine residues in proton transfer reactions (*3, 5, 31–33*). Direct correlation of these functions in bRCs to possible roles in PSI is not possible, as the bRC is a type II RC with terminal quinone acceptors whereas PSI is a type I RC with electron transfer reactions terminating at two iron−sulfur centers (*7, 21*). As in bRC, however, PSI metal sites might help identify histidine residues essential in proton movement coupled to electron transfer on the acceptor side of PSI. Although no proton uptake mechanisms have been invoked for PSI function, counterion movement should accompany charge separation. The presence of histidine ligation, as shown with HYSCORE, and the potential change in histidine ligation upon ferredoxin docking, as shown with XAFS, hint at such possibilities. Furthermore, site-directed mutagenesis of His(D95) has shown the importance of this residue in the increased affinity of PSI for ferredoxin at acidic pH, suggesting that this histidine acts as a proton sensor responding to acidification on the acceptor side of PSI (*25, 26*). Metal binding

experiments on the acceptor side of PSI provide a unique means of further investigating this important pH effect.

Importantly, EPR and XAFS experiments both show the interaction of ferredoxin with the native Cu sites on PSI. The docking of ferredoxin to PSI involves electrostatic interactions of the highly acidic, negatively charged surface of ferredoxin with a basic patch of PSI provided mainly by the PsaD and PsaC subunits (*7*). Site-directed mutations in the PsaC, PsaD, and PsaE stromal subunits of PSI show the importance of net PSI charge on the affinity of ferredoxin for PSI (*9*). For example, single substitution of the highly conserved Glu(D103) by a neutral glutamine resulted in a substantial decrease in the dissociation constant (*26*). Similarly, metal ion binding to negatively charged amino acid residues, i.e., Glu or Asp, would neutralize charge. In this manner, the introduction of a positively charged metal ion binding to the ferredoxin docking region on PSI would change the electrostatic surface charge provided by PSI that is available for the electrostatic "steering" (*26*) and association of ferredoxin. Also, the likely direct ligation by amino acid(s) from ferredoxin to a Cu^{2+} center on PSI, as indicated by XAFS, may well affect the positioning or dissociation constant of ferredoxin.

Native Cu binding sites on PSI could provide a molecular basis for Cu^{2+} inhibition of photosynthesis at high Cu concentrations. Although Cu is an essential micronutrient for photosynthesizing organisms, at high concentrations Cu is an effective inhibitor of photosynthesis for both algae and higher plants (*34*). In PSI, Cu markedly inhibited the ferredoxin-dependent $NADP^+$ reduction, indicating that Cu interferes with electron transport on the reducing side of PSI by a direct interaction with ferredoxin (*35, 36*). We do not know if PSI metal sites inhibit or enhance docking. Either scenario could explain the observed inhibitory effects of Cu, such as saturation of ferredoxin and PSI surfaces with bound Cu inhibiting proper docking or direct ligation of Cu by both ferredoxin and PSI slowing the normal rate of release of ferredoxin following electron transfer.

This work provides the groundwork for future bioinorganic studies aimed at elucidating the involvement of surface metal ion sites in ferredoxin−PSI reactions. Our discovery of native metal ion sites on PSI provides another example of surface metal sites on proteins, demonstrating their involvement in protein–protein interactions. Potentially, these results could lead to the first example of metal ion modulation of interprotein electron transfer between a photosynthetic RC and its soluble reaction partner.

ACKNOWLEDGMENT

We thank A. Wagner for growth of the cyanobacteria and M. C. Thurnauer for critical reading of the manuscript.

REFERENCES

1. Utschig, L. M., Ohigashi, Y., Thurnauer, M. C., and Tiede, D. M. (1998) A new metal-binding site in photosynthetic bacterial reaction centers that modulates Q_A to Q_B electron transfer. *Biochemistry 37*, 8278–8281.
2. Utschig, L. M., and Thurnauer, M. C. (2004) Metal ion modulated electron transfer in photosynthetic proteins. *Acc. Chem. Res. 37*, 439–447.
3. Axelrod, H. L., Abresch, E. C., Paddock, M. L., Okamura, M. Y., and Feher, G. (2000) Determination of the binding sites of the proton transfer inhibitors Cd^{2+} and Zn^{2+} in bacterial reaction centers. *Proc. Natl. Acad. Sci. U.S.A. 97*, 1542–1547.
4. Paddock, M. L., Graige, M. S., Feher, G., and Okamura, M. Y. (1999) Identification of the proton pathway in bacterial reaction centers: Inhibition of proton transfer by binding of Zn^{2+} or Cd^{2+}. *Proc. Natl. Acad. Sci. U.S.A. 96*, 6183–6188.
5. Adelroth, P., Paddock, M. L., Tehrani, A., Beatty, J. T., Feher, G., and Okamura, M. Y. (2001) Identification of the proton pathway in bacterial reaction centers: Decrease of proton transfer rate by mutation of surface histidines at H126 and H128 and chemical rescue by imidazole identifies the initial proton donors. *Biochemistry 40*, 14538–14546.
6. Mulkidjanian, A. Y., Heberle, J., and Cherepanov, D. A. (2006) Protons at interfaces: Implications for biological energy conversion. *Biochim. Biophys. Acta 1757*, 913–930.
7. Jordan, P., Fromme, P., Witt, H. T., Klukas, O., Saenger, W., and Krauss, N. (2001) Three-dimensional structure of cyanobacterial photosystem I at 2.5 Å resolution. *Nature 411*, 909–917.
8. Grotjohann, I., and Fromme, P. (2005) Structure of cyanobacterial Photosystem I. *Photosynth. Res. 2005*, 51–72.
9. Sétif, P., Fisher, N., Lagoutte, B., Bottin, H., and Rochaix, J.-D. (2002) The ferredoxin docking site of photosystem I. *Biochim. Biophys. Acta 1555*, 204–209.
10. Allen, M. B., and Arnon, D. I. (1955) Studies on nitrogen-fixing blue-green algae. I. Growth and nitrogen fixation by Anabaena Cylindrica Lemm. *Plant Physiol. 30*, 366–372.
11. Rögner, M., Nixon, P. J., and Diner, B. A. (1990) Purification and characterization of photosystem I and photosystem II core complexes from wild-type and phycocyanin-deficient strains of the cyanobacterium *Synechocystis* PCC 6803. *J. Biol. Chem. 265*, 6189–6196.
12. Van der Est, A., Bock, C. H., Goldbeck, J. H., Brettel, K., Setif, P., and Stehlik, D. (1994) Electron transfer from the acceptor A_1 to the iron-sulfur centers in photosystem I as studied by transient EPR spectroscopy. *Biochemistry 33*, 11789–11797.
13. Lichtenthaler, H. K. (1987) Chlorophylls and carotenoids: Pigments of photosynthetic biomembranes. *Methods Enzymol. 148*, 350.
14. Markwell, J. P., Thornber, J. P., and Skrdla, M. P. (1980) Effect of detergents on the reliability of a chemical assay for P-700. *Biochim. Biophys. Acta 591*, 391–399.
15. Utschig, L. M., Poluektov, O., Tiede, D. M., and Thurnauer, M. C. (2000) EPR investigation of Cu^{2+}-substituted photosynthetic bacterial reaction centers: Evidence for histidine ligation at the surface metal site. *Biochemistry 39*, 2961–2969.
16. Utschig, L. M., Poluektov, O., Schlesselman, S. L., Thurnauer, M. C., and Tiede, D. M. (2001) Cu^{2+} sites in photosynthetic bacterial reaction centers from *Rhodobacter sphaeroides*, *Rhodobacter capsulatus*, and *Rhodopseudomonas viridis*. *Biochemistry 40*, 6132–6141.
17. Tagawa, K., and Arnon, D. I. (1968) Oxidation-reduction potentials and stoichiometry of electron transfer in ferredoxins. *Biochim. Biophys. Acta 153*, 602–613.
18. Chen, L. X., Utschig, L. M., Schlesselman, S. L., and Tiede, D. M. (2004) Temperature and light-induced structural changes in photosynthetic reaction center proteins probed by X-ray absorption fine structure. *J. Phys. Chem. B 108*, 3912–3924.
19. Peisach, J., and Blumberg, W. E. (1974) Structural implications derived from the analysis of electron paramagnetic resonance spectra of natural and artificial copper proteins. *Arch. Biochem. Biophys. 165*, 691–708.
20. Solomon, E. I., Penfield, K. W., and Wilcox, D. E. (1983) Active sites in copper proteins: An electronic structure overview, in *Structure Bonding (Berlin)*, pp 3–57, Springer-Verlag, Berlin.
21. Vassiliev, I. R., Antonkine, M. L., and Goldbeck, J. H. (2001) Iron-sulfur clusters in type I reaction centers. *Biochim. Biophys. Acta 1507*, 139–160.
22. Höfer, P., Grupp, A., Nebenföhr, H., and Mehring, M. (1986) Hyperfine sublevel correlation (hyscore) spectroscopy: A 2D ESR investigation of the squaric acid radical. *Chem. Phys. Lett. 132*, 279–282.
23. Schweiger, A., and Jeschke, G. (2001) *Principles of Pulse Electron Paramagnetic Resonance*, Oxford University Press, Oxford, U.K.
24. Utschig, L. M., Astashkin, A. V., Raitsimring, A. M., Thurnauer, M. C., and Poluektov, O. G. (2004) Pulsed EPR/ENDOR characterization of the Cu^{2+} surface site in photosynthetic bacterial reaction centers. *J. Phys. Chem. B 108*, 11150–11156.
25. Hanley, J., Sétif, P., Bottin, H., and Lagoutte, B. (1996) Mutagenesis of photosystem I in the region of the ferredoxin cross-linking site: Modifications of positively charged amino acids. *Biochemistry 35*, 8563–8571.

26. Bottin, H., Hanley, J., and Lagoutte, B. (2001) Role of acidic amino acid residues of PsaD subunit on limiting the affinity of photosystem I for ferredoxin. *Biochem. Biophys. Res. Commun. 287*, 833–836.
27. Shadle, S. E., Penner-Hahn, J. E., Schugar, H. J., Hedman, B., Hodgson, K. O., and Solomon, E. I. (1993) X-ray absorption spectroscopic studies of the blue copper site: Metal and ligand K-edge studies to probe the origin of the EPR hyperfine splitting in plastocyanin. *J. Am. Chem. Soc. 115*, 767–776.
28. Binda, C., Coda, A., Aliverti, A., Zanetti, G., and Mattevi, A. (1998) Structure of the mutant E92K of [2Fe-2S] ferredoxin I from *Spinacia oleracea* at 1.7 Å resolution. *Acta Crystallogr. D54*, 1353–1358.
29. Sétif, P. (2001) Ferredoxin and flavodoxin reduction by photosystem I. *Biochim. Biophys. Acta 1507*, 161–179.
30. Fromme, P., Bottin, H., Krauss, N., and Sétif, P. (2002) Crystallization and electron paramagnetic resonance characterization of the complex of photosystem I with its natural electron acceptor ferredoxin. *Biophys. J. 83*, 1760–1773.
31. Adelroth, P., Paddock, M. L., Sagle, L. B., Feher, G., and Okamura, M. Y. (2000) Identification of the proton pathway in bacterial reaction centers: Both protons associated with reduction of Q_B to Q_BH_2 share a common entry point. *Proc. Natl. Acad. Sci. U.S.A. 97*, 13086–13091.
32. Paddock, M. L., Feher, G., and Okamura, M. Y. (2000) Identification of the proton pathway in bacterial reaction centers: Replacement of Asp-M17 and Asp-L210 with Asn reduces the proton transfer rate in the presence of Cd^{2+}. *Proc. Natl. Acad. Sci. U.S.A. 97*, 1548–1553.
33. Gerencser, L., and Maroti, P. (2001) Retardation of proton transfer caused by binding of the transition metal ion to the bacterial reaction center is due to pK_a shifts of key protonatable residues. *Biochemistry 40*, 1850–1860.
34. Droppa, M., and Horvath, G. (1990) The role of copper in photosynthesis. *Crit. Rev. Plant Sci. 9*, 111–123.
35. Shioi, Y., Tamai, H., and Sasa, T. (1978) Effects of copper on photosynthetic electron transport systems in spinach chloroplasts. *Plant Cell Physiol. 19*, 203–209.
36. Shioi, Y., Tamai, H., and Sasa, T. (1978) Inhibition of photosystem II in the green alga *Ankistrodesmus falcutus* by copper. *Physiol. Plant. 44*, 434–440.

BI800038D